

Spin-State Transition and Metal-Insulator Transition in $\text{La}_{1-x}\text{Eu}_x\text{CoO}_3$

J. Baier, S. Jodlauk, M. Kriener, A. Reichl, C. Zobel, H. Kierspel, A. Freimuth, and T. Lorenz
II. Physikalisches Institut, Universität zu Köln, Zùlpicher Str. 77, 50937 Köln, Germany

(Dated: October 2, 2018)

We present a study of the structure, the electric resistivity, the magnetic susceptibility, and the thermal expansion of $\text{La}_{1-x}\text{Eu}_x\text{CoO}_3$. LaCoO_3 shows a temperature-induced spin-state transition around 100 K and a metal-insulator transition around 500 K. Partial substitution of La^{3+} by the smaller Eu^{3+} causes chemical pressure and leads to a drastic increase of the spin gap from about 190 K in LaCoO_3 to about 2000 K in EuCoO_3 , so that the spin-state transition is shifted to much higher temperatures. A combined analysis of thermal expansion and susceptibility gives evidence that the spin-state transition has to be attributed to a population of an intermediate-spin state without orbital degeneracy for $x < 0.5$ and with orbital degeneracy for larger x . In contrast to the spin-state transition, the metal-insulator transition is shifted only moderately to higher temperatures with increasing Eu content, showing that the metal-insulator transition occurs independently from the spin-state distribution of the Co^{3+} ions. Around the metal-insulator transition the magnetic susceptibility shows a similar increase for all x and approaches a doping-independent value around 1000 K indicating that well above the metal-insulator transition the same spin state is approached for all x .

I. INTRODUCTION

LaCoO_3 has unusual physical properties, which have attracted continuing interest for decades.¹ Nevertheless, the magnetic, electronic, and structural properties of this compound remain the subject of controversial discussion. The magnetic susceptibility χ shows a maximum around 100 K that is usually ascribed to a spin-state transition from a nonmagnetic insulating state at low temperatures to a paramagnetic insulating state at higher temperatures.^{2,3,4,5,6,7,8,9,10,11} In addition, around 500 K a metal-insulator transition occurs,^{12,13} which is accompanied by an increase of the magnetic moment leading to a broad plateau in the magnetic susceptibility.^{14,15} The Co^{3+} ions may occur in three different spin states, the low-spin (LS) ($t_{2g}^6 e_g^0$, $S = 0$), the intermediate-spin (IS) ($t_{2g}^5 e_g^1$, $S = 1$), and the high-spin (HS) state ($t_{2g}^4 e_g^2$, $S = 2$). The energies of these spin states depend on the balance between the crystal field splitting (Δ_{CF}) and the Hund's rule coupling (J_{H}). A multiplet calculation for a $3d^6$ configuration in a cubic crystal field yields that the ground state is either the LS (large Δ_{CF}) or the HS state (large J_{H}), but never the IS state.¹⁶ Therefore, in earlier publications the spin-state transition was often attributed to a thermal population of the HS state from the LS ground state.^{2,4,5,12,14} However, a population of the HS state should result in a susceptibility that is much larger than observed experimentally.¹⁵ More recent investigations^{7,8,9,10,11,15,17} favor a LS/IS scenario, which yields a quantitative description of $\chi(T)$ and which also explains an experimentally observed scaling behavior between $\chi(T)$ and the thermal expansion $\alpha(T)$.¹⁵ From a theoretical point of view the LS/IS scenario is supported by the results of LDA+U calculations (where LDA stands for the local density approximation), which yield that the IS state may be stabilized by a hybridization between Co e_g and O $2p$ levels.^{6,18} Nevertheless, the question of which spin state is populated is not yet clarified unambiguously.

Based on high-field electron spin resonance (ESR) data the population of a spin-orbit coupled HS state with a total angular momentum $\tilde{j} = S - \tilde{l} = 1$ has been suggested recently.¹⁹ Here, $\tilde{l} = 1$ denotes the effective orbital momentum arising from the partial occupation of the t_{2g} orbital. However, this ESR result is in conflict with the susceptibility data, because the ESR data yield a g factor of about 3.5 which leads to a magnetic susceptibility that is about three times larger than that observed experimentally.

Within the originally proposed LS/HS scenario the reduced absolute value of the susceptibility has been traced back to an ordering of LS and HS Co^{3+} ions. Moreover, this ordering was used to explain that despite the partial occupation of e_g states above the spin-state transition around 100 K LaCoO_3 remains insulating up to about 500 K and the metal-insulator transition was attributed to a melting of this order. However, no experimental evidence for such a LS/HS superstructure has been reported so far. Within the LS/IS scenario the occurrence of orbital order which remains stable up to 500 K has been proposed as a cause why the metal-insulator transition and the spin-state transition do not coincide.⁶ Experimental evidence for orbital order stems from changes of phonon modes measured by optical spectroscopy¹⁰ and from a pair density function analysis of pulsed neutron data²⁰. More recently, a high-resolution single crystal x-ray study of LaCoO_3 has revealed a small monoclinic distortion that is related to the Jahn-Teller (JT) effect of the thermally excited Co^{3+} ions in the IS state.²¹ Indirect evidence for this scenario is also obtained from the scaling between $\chi(T)$ and $\alpha(T)$ around the spin-state transition,¹⁵ which requires that the orbital degeneracy of the IS state is lifted as it is the case for JT-distorted CoO_6 octahedra. Moreover, a suppression of the JT distortion in the metallic phase should restore the orbital degeneracy and thus could partially explain the enhanced magnetic susceptibility above the metal-

insulator transition.¹⁵ Alternative explanations of the enhanced susceptibility in the metallic phase rely on scenarios which include all three different spin states, assuming that the IS state is populated around the spin-state transition and the HS state becomes populated at the metal-insulator transition.^{8,9,17}

In order to get more insight to the spin-state transition of LaCoO_3 and its relation to the metal-insulator transition we present an experimental study of the structural changes, the magnetic susceptibility, the electrical resistivity, and the thermal expansion of $\text{La}_{1-x}\text{Eu}_x\text{CoO}_3$ with $0 \leq x \leq 1$. The basic idea is that the partial substitution of La^{3+} by the smaller Eu^{3+} systematically increases the chemical pressure which should enhance the crystal field splitting and therefore stabilize the low-spin state. We have chosen the substitution by Eu^{3+} because it has a vanishing total angular momentum J of the 4f shell. Using other rare earth ions with finite J would strongly hamper the analysis of the Co^{3+} magnetism. Our main findings are as follows: (i) With increasing Eu content the spin-state transition is drastically shifted towards higher temperatures. (ii) We observe a scaling behavior between the magnetic susceptibility and the thermal expansion, which gives clear evidence that for low temperatures ($T < 200$ K) and low Eu content ($x \leq 0.25$) the spin-state transition arises from a thermal population of the IS state without orbital degeneracy. The lack of orbital degeneracy can be interpreted as orbital order or as a consequence of JT distortions of the CoO_6 octahedra with Co^{3+} in the JT-active IS state²². In addition, we find some indication that there is an orbital degeneracy of the IS state for $x > 0.5$. (iii) All samples are good insulators below 400 K. The electrical resistivity behaves like $\rho \propto \exp(\Delta_{\text{act}}/T)$, with an activation energy Δ_{act} that strongly increases with Eu content. (iv) The metal-insulator transition is shifted only moderately to higher temperatures T_{MI} with increasing Eu content, much weaker than that of the spin-state transition. This shows that T_{MI} is only weakly influenced by the thermal population of the IS state. (v) For all Eu concentrations the metal-insulator transition is accompanied by an increase of χ of about $5 \cdot 10^{-4}$ emu/mole and the susceptibility approaches a common value for $T \rightarrow 1000$ K indicating a common spin state. The nature of this high-temperature spin state remains, however, unclear, because it cannot be deduced from an analysis of the susceptibility data alone.

II. EXPERIMENT

We prepared crystals of $\text{La}_{1-x}\text{Eu}_x\text{CoO}_3$ with $x = 0, 0.1, 0.15, 0.2, 0.25, 0.5, 0.75$, and 1 by the floating zone method in a four-mirror image furnace. The preparation parameters are essentially the same as those described in Ref. 23 for the growth of $\text{La}_{1-x}\text{Sr}_x\text{CoO}_3$ single crystals. The LaCoO_3 single crystal studied here is the same as used in Refs. 15,23. The stoichiometry of the crys-

tals has been checked by energy-dispersive x-ray analysis. All samples are single phase as has been confirmed by x-ray powder diffraction at room temperature. From Laue photographs of both ends of the crystals we have found that LaCoO_3 and EuCoO_3 are single crystals, whereas the samples with $0 < x < 1$ are polycrystalline. The electrical resistivity has been measured by a standard four-probe technique on bar-shaped samples of typical dimensions of $2 \times 3 \times 5 \text{ mm}^3$. Wires have been attached by conductive silver epoxy to four gold stripes, which have been evaporated on the sample surface. We have used a dc technique for resistivity values above 1Ω and an ac technique in the sub- Ω range. The susceptibility measurements have been performed between 4 and 300 K in a field of 0.05 T using a superconducting quantum interference device magnetometer (*Cryogenic*, S600X) and in the temperature range from 200 to 1000 K in a field of 1 T with a home-built Faraday balance. High-resolution measurements of the linear thermal expansion were performed using a home-built capacitance dilatometer in the temperature range from 4 to 180 K.²⁴

III. RESULTS

The results of our room temperature powder x-ray diffraction measurements of $\text{La}_{1-x}\text{Eu}_x\text{CoO}_3$ are summarized in Table I. With increasing Eu content, the cell volume per formula unit shrinks almost linearly by about 6% from 56 \AA^3 in LaCoO_3 to 52.75 \AA^3 in EuCoO_3 . Between $x = 0.2$ and 0.25 the symmetry changes from rhombohedral ($R\bar{3}c$) to orthorhombic ($Pnma$), as it is typical for perovskites when the tolerance factor $t = (\langle r_A \rangle + r_O)/(\sqrt{2}(r_{\text{Co}} + r_O))$ decreases. Here r_{Co} and r_O denote the ionic radii of the Co^{3+} and O^{2-} ions, respectively, and $\langle r_A \rangle = (1-x)r_{\text{La}} + xr_{\text{Eu}}$ is the average radius of the A site ions, i. e. the average radius of La^{3+} and Eu^{3+} . Such a symmetry change from rhombohedral to orthorhombic has also been observed in $\text{La}_{1-x}\text{Ca}_x\text{CoO}_3$ for $x \geq 0.2$.^{23,25}

TABLE I: Room temperature lattice constants and volume per formula unit of $\text{La}_{1-x}\text{Eu}_x\text{CoO}_3$. The symmetry is rhombohedral ($R\bar{3}c$) for $x \leq 0.2$ and orthorhombic ($Pnma$) for $x \geq 0.25$.

x	$a_{\text{R}} (\text{\AA})$	$\alpha_{\text{R}} (\text{^\circ})$	$a (\text{\AA})$	$b (\text{\AA})$	$c (\text{\AA})$	$V (\text{\AA}^3/\text{f.u.})$
0	5.379	60.8°				56.02
0.1	5.367	60.9°				55.76
0.15	5.393	60.4°				55.99
0.2	5.387	60.3°				55.60
0.25			5.409	7.611	5.370	55.25
0.5			5.353	7.565	5.344	54.10
0.75			5.357	7.531	5.314	53.60
1			5.370	7.477	5.255	52.75

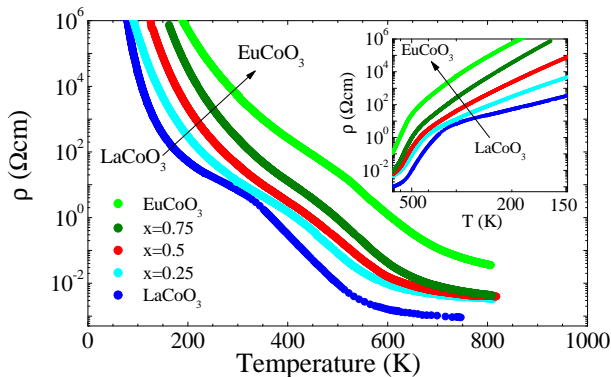


FIG. 1: Electrical resistivity of $\text{La}_{1-x}\text{Eu}_x\text{CoO}_3$ as a function of temperature for different x . The inset shows the same data on a reciprocal temperature scale.

A. Resistivity

In Fig. 1 we present the electrical resistivity ρ of $\text{La}_{1-x}\text{Eu}_x\text{CoO}_3$. All samples studied are insulators. We find a systematic increase of ρ with increasing Eu content. Qualitatively, such an increase may be expected from the decreasing tolerance factor. When t decreases, the deviation of the Co-O-Co bond angle from 180° increases and therefore the hopping probability of charge carriers decreases. In accord with Refs. 13,14,26,27 the resistivity of LaCoO_3 shows an activated behavior ($\rho \propto \exp(\Delta_{\text{act}}/T)$) below 400 K with an activation energy $\Delta_{\text{act}} \simeq 1200$ K (see also Ref. 23). Above 400 K a steep decrease of the resistivity takes place, which is, according to optical conductivity data¹³, attributed to a metal-insulator transition around 500 K. Note that above this transition LaCoO_3 remains a rather poor metal with a resistivity of about 1 m Ωcm . The Eu-doped samples show similar $\rho(T)$ curves. As shown in the inset of Fig. 1 the slopes of the $\log(\rho)$ versus T^{-1} , i. e. Δ_{act} , curves strongly increase with increasing Eu content. The onset of the steep decrease of $\rho(T)$ is shifted to higher temperatures with increasing x , signaling that the metal-insulator transition is shifted to higher temperatures.²⁸ However, the shift of the transition temperature T_{MI} is much weaker than that of Δ_{act} . As will be shown later (Fig. 5) Δ_{act} increases by about a factor of 3 and T_{MI} only by about 25% from $x = 0$ to 1. Such a different increase of Δ_{act} and T_{MI} has also been found in resistivity measurements on $R\text{CoO}_3$ with $R = \text{La}, \dots, \text{Gd}$.²⁹

B. Magnetic susceptibility

In Fig. 2 we compare the magnetic susceptibility of LaCoO_3 and of EuCoO_3 . In order to extract the Curie susceptibility of the Co^{3+} ions from the raw data we subtract a background contribution consisting of (1) a Curie-Weiss contribution $\chi_{\text{imp}} = \frac{C}{T-\Theta}$ due to magnetic impurities and/or oxygen nonstoichiometry, (2) a temperature-

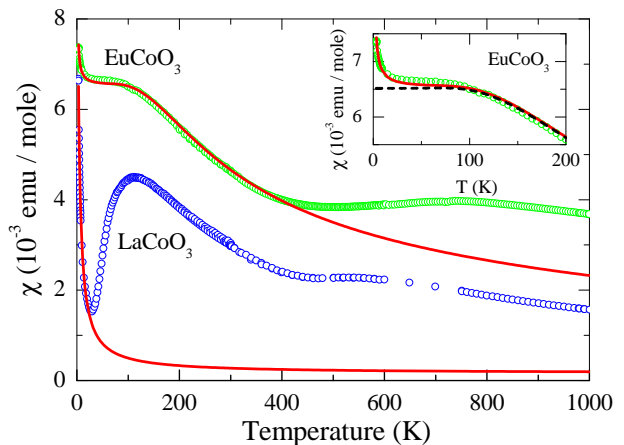


FIG. 2: Magnetic susceptibility of EuCoO_3 and LaCoO_3 as a function of temperature (symbols) together with fits (solid lines) of the respective background contributions (Eq. 1). The inset shows an expanded view of the low-temperature susceptibility of EuCoO_3 , which is almost entirely given by the Eu^{3+} van Vleck contribution shown by the dashed line.

independent contribution χ_0 due to the diamagnetism of the core electrons and the van Vleck susceptibility of the Co^{3+} ions,³⁰ and (3) the van Vleck susceptibility $\chi_{\text{vV}}^{\text{Eu}}$ of the Eu^{3+} ions weighted by the Eu content x . Note that it is *a priori* not clear that in $\text{La}_{1-x}\text{Eu}_x\text{CoO}_3$ all Eu ions are three-valent. However, due to the $4f^7$ configuration of divalent Eu^{2+} with $S = 7/2$ its presence would cause a strong increase of the Curie-Weiss contribution χ_{imp} . Since this is not at all the case in our samples, we conclude that the amount of Eu^{2+} is negligibly small. The temperature dependence of the van Vleck susceptibility of Eu^{3+} ions is well known and depends solely on the energy gap Δ_{Eu} between the $J = L - S = 0$ ground state and the $J = 1$ first excited state of the $4f^6$ multiplet of Eu^{3+} .³¹ The gap Δ_{Eu} is typically of the order of 500 K. The entire background susceptibility of $\text{La}_{1-x}\text{Eu}_x\text{CoO}_3$ can thus be written as

$$\chi_{\text{bg}}(T) = \frac{C}{T-\Theta} + \chi_0 + x \cdot \chi_{\text{vV}}^{\text{Eu}}(\Delta_{\text{Eu}}, T). \quad (1)$$

The parameters C , Θ , χ_0 , and Δ_{Eu} are determined by nonlinear least-square fits of χ_{bg} to the low-temperature data, where the Co^{3+} ions are in the nonmagnetic LS state. As shown in Fig. 2, χ_{bg} describes the low-temperature $\chi(T)$ up to about 25 K for LaCoO_3 and about 400 K for EuCoO_3 .³² This implies that the Co^{3+} ions remain essentially in the LS state up to these temperatures, respectively.

In the upper panel of Fig. 3 we show the susceptibility of $\text{La}_{1-x}\text{Eu}_x\text{CoO}_3$ for $0 \leq x \leq 1$. When the Eu content increases the susceptibility at low temperatures becomes more and more dominated by the Eu^{3+} van Vleck contribution. We have fitted the respective low-temperature $\chi(T)$ data by Eq. (1) for all samples and summarized the fit parameters in Table II. We find $\Delta_{\text{Eu}} \simeq 460$ K (Ref. 33) and for the impurity contribution we have obtained $C \simeq$

0.02 emuK/mole and $\Theta \simeq -3$ K corresponding to impurity concentrations of less than 1% (see Ref. 15) with weak antiferromagnetic interaction. For the sum of core diamagnetism and Co^{3+} van Vleck paramagnetism we find $0 \leq \chi_0 \leq 1.6 \cdot 10^{-4}$ emu/mole. In our previous analysis of $\chi(T)$ of LaCoO_3 we have used slightly different parameters, namely $\chi_0 = 6.5 \cdot 10^{-4}$ emu/mole, $C = 0.02$ emuK/mole and $\Theta = 0$.¹⁵ The main difference concerns the smaller value of χ_0 , which we use in the present analysis for the following reason: The low-temperature $\chi(T)$ data of all $\text{La}_{1-x}\text{Eu}_x\text{CoO}_3$ samples with $x > 0$ can be well reproduced only for $\chi_0 \leq 10^{-4}$ emu/mole. Since it appeared very unlikely that χ_0 is significantly larger for $x = 0$ than for all samples with $x > 0$, we have measured the magnetization of LaCoO_3 at 1.8 K up to 14 T. This field is sufficient to saturate the impurity contribution of the magnetization and the remaining slope of $M(H)$ in the high-field region, e.g. for $H \geq 11$ T where $\mu_B H/k_B T \geq 4$, is then given by $dM/dH \simeq \chi_0$. For LaCoO_3 , this method yields $\chi_0 = 1.6 \cdot 10^{-4}$ emu/mole, which is a much more reliable measure of χ_0 than the fit of the low-temperature susceptibility data by Eq. (1) because of the rather restricted low-temperature range for $x = 0$ ($T \lesssim 25$ K).

In the lower panel of Fig. 3 we show the Curie susceptibility of the Co^{3+} ions after subtracting χ_{bg} from the raw data. The susceptibility of LaCoO_3 shows a low-temperature maximum due to the spin-state transition and a high-temperature shoulder around the metal-insulator transition. With increasing Eu content the low-temperature maximum is continuously suppressed and strongly shifted to higher temperatures, whereas the high-temperature shoulder moves only moderately to higher temperatures corresponding to the weak increase of T_{MI} with x inferred from $\rho(T)$. For $x < 0.75$ two separate anomalies are clearly seen in the $\chi_{\text{Co}}(T)$ curves, while in EuCoO_3 these anomalies have finally merged into one broad increase of $\chi(T)$. It is remarkable that after the subtraction of χ_{bg} the susceptibility data of all samples approach a value of about $1.4 \cdot 10^{-3}$ emu/mole for $T \rightarrow 1000$ K.

TABLE II: Fit parameters of the background susceptibility $\chi_{\text{bg}}(T)$ (see Eq. 1),³³ which describes the low-temperature data of the measured susceptibility.

Eu content	χ_0 ($10^{-4} \frac{\text{emu}}{\text{mole}}$)	C ($\frac{\text{emuK}}{\text{mole}}$)	Θ (K)	Δ_{Eu} (K)
LaCoO_3	1.6	0.034	-2.2	-
$x = 0.1$	0	0.046	-3.4	460
$x = 0.15$	1.0	0.022	-2.8	460
$x = 0.2$	1.0	0.016	-2.1	460
$x = 0.25$	1.0	0.012	-2.8	460
$x = 0.5$	0.3	0.01	0	462
$x = 0.75$	0	0.012	0	473
EuCoO_3	0	0.003	0	457

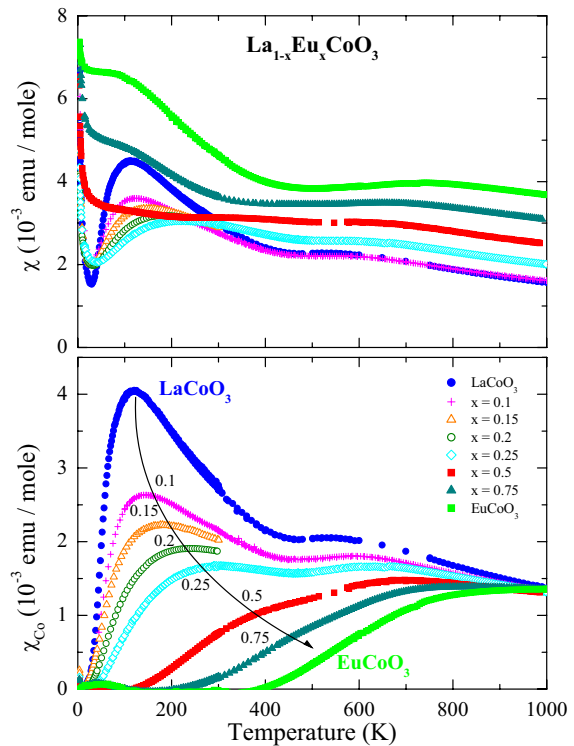


FIG. 3: The upper panel presents the magnetic susceptibility of $\text{La}_{1-x}\text{Eu}_x\text{CoO}_3$ as a function of temperature. With increasing Eu content the susceptibility at low temperatures is more and more dominated by the van Vleck contribution of the Eu^{3+} ions. The lower panel shows the Curie susceptibility of the Co^{3+} ions after subtracting a background susceptibility according to Eq. 1 (see text).

Without further quantitative analysis the data in the lower panel of Fig. 3 clearly show that the spin-state transition is systematically shifted towards higher temperatures with increasing Eu content. Similar to physical pressure in LaCoO_3 ,^{34,35} the chemical pressure imposed by Eu stabilizes the LS state of the Co^{3+} ions due to the enhanced crystal-field splitting. This conclusion agrees with the results of Co nuclear magnetic resonance (NMR) studies on $R\text{CoO}_3$ with $R = \text{La}, \dots, \text{Eu}$.^{36,37} A quantitative analysis of $\chi_{\text{Co}}(T, x)$ and its relation to the metal-insulator transition will be given below.

C. Thermal expansion

In Fig. 4 we present high-resolution measurements of the linear thermal expansion α of $\text{La}_{1-x}\text{Eu}_x\text{CoO}_3$. As shown in Ref. 15, α is a very sensitive probe of the spin-state transition. In LaCoO_3 α steeply increases above about 25 K and reaches a maximum around 50 K. This unusual behavior can be attributed to the spin-state transition, which leads to a thermal population of the e_g or-

bitals. Since the e_g orbitals are oriented towards the surrounding negative O^{2-} ions, this causes an anomalous, additional contribution $\Delta\alpha$ to the lattice expansion. As reported in Ref. 15 the thermal expansion and the magnetic susceptibility fulfill the scaling relation

$$C \cdot \Delta\alpha(T) = \frac{\partial(\chi_{Co} \cdot T)}{\partial T} \quad (2)$$

with a scaling factor C depending on the spin state of the excited state. For $LaCoO_3$, we find C *simeq* 195 emu K/mole, which agrees very well with the value expected for a population of the IS state without orbital degeneracy (190 emu K/mole) and strongly deviates from the values of other scenarios such as a population of the IS state with orbital degeneracy (290 emu K/mole) or a thermal population of the HS state with (1000 emu K/mole) and without orbital degeneracy (690 emu K/mole), respectively.^{15,38}

The raw thermal expansion data of $La_{1-x}Eu_xCoO_3$ shown in the upper panel of Fig. 4 reveal an anomalous thermal expansion of the samples with $x \leq 0.25$, which systematically flattens and shifts towards higher temperatures with increasing x . In contrast, the $\alpha(T)$ curves of the samples with $x \geq 0.5$ are essentially identical and do not show any anomalous behavior up to 180 K. It is therefore reasonable to use the average of these curves as a background α_{bg} representing the normal lattice expansion, which is present irrespective of the spin-state transition. The anomalous thermal expansion for $x < 0.5$ is then obtained by $\Delta\alpha = \alpha - \alpha_{bg}$.³⁹ As shown in the lower panel of Fig. 4 we find that for all samples with Eu contents $0 \leq x \leq 0.25$ the scaling relation between thermal expansion and magnetic susceptibility [Eq. (2)] is well fulfilled. The scaling factors for the different samples lie in the range from 190 to 210 emu K/mole and agree well with the value expected for a population of the IS state without orbital degeneracy and deviate strongly from other possible scenarios (see Table III). Thus, we conclude that, just as in $LaCoO_3$, the spin-state transition in $La_{1-x}Eu_xCoO_3$ for $x \leq 0.25$ arises from a thermal population of the IS state without orbital degeneracy. With increasing Eu content the spin gap is enhanced and the spin-state transition is therefore shifted towards higher temperatures.

IV. DISCUSSION

In Fig. 5 we compare the Curie susceptibility of the Co^{3+} ions obtained from the raw data after subtracting χ_{bg} [see Eq. (1) and Table II] and the resistivity which is presented in the form $\frac{d \ln \rho}{d(T-1)}$. If this latter quantity is constant, ρ follows an activated behavior $\rho \propto \exp(\Delta_{act}/T)$ with a constant activation energy $\Delta_{act} = \frac{d \ln \rho}{d(T-1)}$. At low temperatures activated behavior is indeed observed. The broad peak of $\frac{d \ln \rho}{d(T-1)}$ at higher temperatures arises from the strong decrease

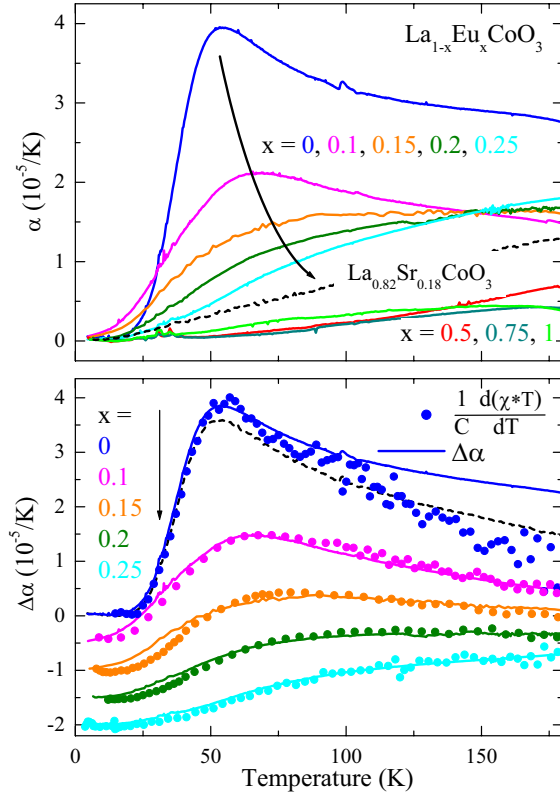


FIG. 4: (Upper panel) Thermal expansion α of $La_{1-x}Eu_xCoO_3$ (solid lines) and $La_{0.82}Sr_{0.18}CoO_3$ (dashed line). (Lower panel) Anomalous thermal expansion $\Delta\alpha = \alpha - \alpha_{bg}$ of $La_{1-x}Eu_xCoO_3$ for $0 \leq x \leq 0.25$ (solid lines), where the averaged α of $La_{1-x}Eu_xCoO_3$ with $0.5 \leq x \leq 1$ has been used as α_{bg} . The dashed line shows $\Delta\alpha$ of $LaCoO_3$ which was analysed in Ref. 15 using α of $La_{0.82}Sr_{0.18}CoO_3$ as α_{bg} . The symbols (\bullet) are obtained from the Co^{3+} susceptibility data (see lower panel of Fig. 3) via the scaling relation $C \cdot \Delta\alpha(T) = \partial(\chi_{Co} \cdot T) / \partial T$ with scaling factors C between 190 and 210 emuK/mole (see Table III). For clarity, the curves for different Eu contents have been shifted by $-0.5 \cdot 10^{-5}/K$ with respect to each other.

of ρ at the metal-insulator transition. We find an almost linear increase of the peak position, i. e. the metal-insulator transition temperature T_{MI} , with increasing x from $T_{MI} \simeq 480$ K in $LaCoO_3$ to $T_{MI} \simeq 600$ K in $EuCoO_3$. For $LaCoO_3$ $\Delta_{act} \simeq 1200$ K is constant below room temperature. With increasing x we find that Δ_{act} deviates more and more from being constant for $T < T_{MI}$. This implies that for the samples with larger resistivities the charge transport deviates from simple activated behavior. Possibly it changes towards variable range hopping, but the temperature range of our $\rho(T)$ curves is too restricted to analyze this in more detail. If we ignore this deviation and consider the room temperature values of Δ_{act} as a measure of an effective activation energy, we find a strong increase of Δ_{act} from

TABLE III: Experimental results of the scaling factors C in the scaling relation $C \cdot \Delta\alpha(T) = \partial(\chi_{\text{Co}} \cdot T) / \partial T$ between anomalous thermal expansion $\Delta\alpha$ and magnetic susceptibility χ for different Eu contents x (see Fig. 4). As shown in Ref. 15 the expected values are $C \simeq 190$ emu K/mole for a thermal population of the IS state without orbital degeneracy and $\simeq 290$ emu K/mole for the IS state with orbital degeneracy. For a population of the HS state with and without orbital degeneracy the expected values amount to 1000 and 690 emu K/mole, respectively³⁸.

x	0	0.1	0.15	0.2	0.25
C (emuK/mole)	195	205	210	210	190

1200 K for LaCoO_3 to about 3400 K for EuCoO_3 . Obviously, the relative increase of the activation energy is much more pronounced than that of the transition temperature (see Table IV) as has also been observed in RCoO_3 .²⁹ In optical conductivity data a strong similarity between the temperature-induced metal-insulator transition of LaCoO_3 and the doping-induced metal-insulator transition in $\text{La}_{1-x}\text{Sr}_x\text{CoO}_3$ has been found.¹³ From this similarity and the anomalously small T_{MI} compared to Δ_{act} it has been concluded that the temperature-induced metal-insulator transition of LaCoO_3 should be viewed as a Mott transition of a strongly correlated electron system.^{13,29}

Inspecting the susceptibility data in Fig. 5 we observe that the metal-insulator transition of $\text{La}_{1-x}\text{Eu}_x\text{CoO}_3$ is always accompanied by an increase of χ . This is obvious for the samples with $x < 0.75$ where the spin-state transition and the metal-insulator transition are well separated, whereas it is less obvious for larger x , since the increase of χ due to the spin-state transition and due to metal-insulator transition are superposed. In order to describe the susceptibility behavior of LaCoO_3 , various models have been considered. For the 100 K spin-state transition a thermal population of the HS or of the IS state has been proposed and for both scenarios different orbital degeneracies ν have been assumed for the excited state (HS: $\nu = 1$ or 3; IS: $\nu = 1, 3$, or 6).^{8,9,10,14,17} In order to also describe the change of χ around the metal-insulator transition even three-state scenarios (LS/IS/HS) with different orbital degeneracies of the excited states have been used.^{8,9,17} In some cases a temperature dependence of the energies of the different spin states has also been considered, which can arise from the thermal expansion and/or from collective interactions between the excited states.^{9,17,40,41}

As mentioned above the scaling between the thermal expansion and the magnetic susceptibility (see Fig. 4 and Table III) gives clear evidence for a thermal population of the IS state with $\nu = 1$ and discards other two-state scenarios.¹⁵ This unambiguous conclusion from the scaling analysis is only possible for $x \leq 0.25$ where the spin-state transition occurs at low enough temperatures. However, we will also use this scenario as a starting point

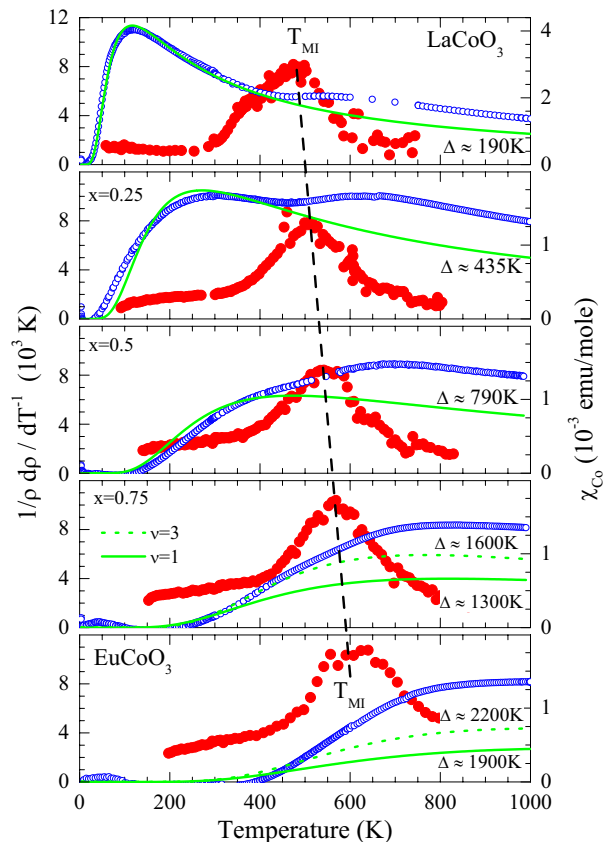


FIG. 5: Curie susceptibility of the Co^{3+} ions (open circles, right y axis) in comparison with the temperature dependence of the activation energy $\Delta_{\text{act}} \simeq \frac{d \ln \rho}{d(T-1)}$ (filled circles, left y axis). The peak of Δ_{act} signals the metal-insulator transition, which slightly shifts towards higher temperatures as marked by the dashed vertical line. The solid (dashed) lines are fits of $\chi_{\text{Co}}(T)$ sufficiently below T_{MI} within a LS/IS scenario with $\nu = 1$ ($\nu = 3$) (see Eq. 3 and text).

for larger x and higher temperatures. In order to derive the energy splitting Δ between the LS and IS state for the different Eu concentrations we have fitted the respective $\chi_{\text{Co}}(T)$ by the susceptibility of a two-level system:

$$\chi(T) = \frac{N_A g^2 \mu_B^2 S(S+1)}{3k_B T} \frac{\nu(2S+1)e^{-\Delta/T}}{1 + \nu(2S+1)e^{-\Delta/T}}. \quad (3)$$

The first fraction describes the Curie susceptibility of the excited state and the second one its thermal population with the Avogadro number N_A , the Bohr magneton μ_B , and the Boltzmann constant k_B , $\nu = 1$ and $S = 1$ denote the orbital degeneracy and the spin of the IS state, which are kept fixed and the g factor is kept close to $g \simeq 2$.

The fit parameters are summarized in Table IV and the corresponding fit curves are shown as solid lines in Fig. 5. The fits describe the experimental data reasonably well up to about 450 K for $x \leq 0.5$. For larger x the agreement between the fits and the experimental data becomes worse, in particular for EuCoO_3 . Because fits

TABLE IV: Activation energy Δ_{act} , metal-insulator transition temperature T_{MI} , energy splitting Δ between the LS and IS states, and g factor of the IS state for different Eu contents (see Fig. 5). Δ_{act} and T_{MI} are deduced from the room temperature value and the maximum of $\frac{d \ln \rho}{d(T-1)}$, respectively. Δ and g are obtained from fits of $\chi_{\text{Co}}(T)$ in the temperature range below the metal-insulator transition within a LS/IS scenario; for $x \leq 0.5$ (≥ 0.75) an IS state without (with) orbital degeneracy has been considered. The last column contains the average energy gaps $\langle \Delta(T) \rangle$ for $T < 400$ K obtained from the experimental data via Eq. 4 with $g = 2.4$ (see Fig. 6.) For $x \geq 0.75$ the values of Δ and $\langle \Delta(T) \rangle$ are only rough estimates, because $\chi_{\text{Co}}(T)$ essentially vanishes in the respective low-temperature range and the agreement between the fits and the experimental data is rather weak.⁴²

Eu content	Δ_{act} (K)	T_{MI} (K)	g	Δ (K)	$\langle \Delta(T) \rangle$ (K)
LaCoO ₃	1200	480	2.28	188	230
$x = 0.1$			2.10	240	300
$x = 0.15$			2.10	270	330
$x = 0.2$			2.10	330	380
$x = 0.25$	2000	510	2.24	435	480
$x = 0.5$	2800	550	2.3	790	840
$x = 0.75$	3200	570	2.4	1600	> 1600
EuCoO ₃	3400	600	2.4	1900	> 2200

with $\nu = 3$ yield somewhat better results with larger gaps ($\Delta \simeq 1600$ and 2200 K for $x = 0.75$ and 1 , respectively) one may speculate that the orbital degeneracy is larger for $x \geq 0.75$. As mentioned above the lifting of the orbital degeneracy in LaCoO₃ arises from a JT effect of the excited Co³⁺ ions in the IS state.^{15,21} Since the spin-state transition takes place at much higher temperatures for $x \geq 0.75$, the JT effect could play a minor role in these samples, since it is reduced by thermal fluctuations. Moreover, the spin-state transition sets in so close to the metal-insulator transition that the JT effect can hardly develop, since above T_{MI} it will be reduced anyway due to the enhanced charge-carrier mobility. Independent of the choice of ν we find a drastic increase of the energy gap Δ with increasing Eu content. We interpret this increase as a consequence of the reduced unit-cell volume due to the Eu substitution causing an enhanced crystal-field splitting which stabilizes the LS relative to the IS state. In Refs. 6,7,18 it has been argued that the IS state of Co³⁺ can be stabilized by a hybridization between the Co $3d$ and the O $2p$ states. Thus, the increase of Δ may, in addition, be enhanced by the decreasing Co $3d$ O $2p$ hybridization with increasing Eu concentration, which is also reflected by the enhanced resistivity (see Fig. 1).

Before discussing the susceptibility data for higher temperatures let us compare the influence of Eu substitution on the spin-state transition and the metal-insulator transition. Obviously, the spin-state transition is shifted much stronger to higher temperatures than the metal-insulator transition. This gives clear ev-

idence that the occurrence of the metal-insulator transition in La_{1-x}Eu_xCoO₃ is independent from the population of the IS state of the Co³⁺ ions. For example, at $T_{\text{MI}} \simeq 480$ K LaCoO₃ has almost a 3:1 distribution between the IS and LS states according to their different degeneracies, whereas in EuCoO₃ the spin-state transition just starts above 400 K so that the population of the IS state in EuCoO₃ around $T_{\text{MI}} \simeq 600$ K is as low as that in LaCoO₃ around 50 K. In this respect the spin-state transition and the metal-insulator transition are decoupled from each other. The observation that for all Eu concentrations $\chi_{\text{Co}}(T)$ seems to approach a common value for $T \rightarrow 1000$ K indicates, however, that for temperatures well above the metal-insulator transition the same spin state (or combination of spin states) is approached in La_{1-x}Eu_xCoO₃ for all x .

As shown in Fig. 5 $\chi_{\text{Co}}(T)$ calculated for the LS/IS scenario underestimates the susceptibility for $T \rightarrow T_{\text{MI}}$. Notably, well above T_{MI} the deviations between the extrapolations of the low-temperature fit curves and the experimental data amount to about $5 \cdot 10^{-4}$ emu/mole for all x (if $\nu = 3$ is used for $x \geq 0.75$). In LaCoO₃ a well-defined anomaly in the specific heat C has been observed around T_{MI} ,⁴³ showing that the metal-insulator transition represents a real phase transition, in contrast to the spin-state transition, which is a thermal population of the excited IS state above the LS state causing only a broad Schottky-type anomaly of C (and α) over a large temperature interval. Consequently, the parameters (or even the model) for the description of $\chi_{\text{Co}}(T)$ above and below T_{MI} can be very different. In principle, there are various sources for an enhanced susceptibility in the metallic phase. As mentioned above the charge-carrier mobility above T_{MI} should melt or at least reduce an orbital order of the IS. Therefore, it is reasonable to use an orbital degeneracy $\nu = 3$ above T_{MI} in Eq. (3), which causes an increase of $\chi_{\text{Co}}(T)$.^{15,38} However, this effect is not sufficient to describe the enhanced susceptibility above T_{MI} as can be clearly seen from the dashed lines calculated with $\nu = 3$ in the lower panels of Fig. 5. From the observation that charge-carrier doped La_{1-x}M_xCoO₃ ($M = \text{Ca}, \text{Sr}, \text{and Ba}$) has a ferromagnetic, metallic ground state above a certain doping level,²³ one may also speculate that an additional increase of $\chi_{\text{Co}}(T)$ could arise from a ferromagnetic coupling above T_{MI} . However, LaCoO₃ above T_{MI} is not directly comparable to La_{1-x}M_xCoO₃, because the ferromagnetic coupling in La_{1-x}M_xCoO₃ arises from a double exchange between Co³⁺ and Co⁴⁺ ions, whereas in LaCoO₃ formally only Co³⁺ ions are present.

A different source of an enhancement of $\chi_{\text{Co}}(T)$ could arise from a partial occupation of the HS state above T_{MI} . Based on this assumption describing the susceptibility of LaCoO₃ within a LS/IS/HS scenario has been attempted.^{8,9,17} However, even within this three-state model the susceptibility of LaCoO₃ is only reproduced if the energies of the IS and the HS state change with temperature. Within this model a nearly temperature-independent $\Delta_{\text{IS}} \simeq 250$ K and a strong decrease for Δ_{HS}

from about 1400 to about 200 K occurring around T_{MI} has been reported for LaCoO_3 .⁹ Here, Δ_{IS} (Δ_{HS}) denote the energy between the LS and the IS (HS) states. Due to the large value of Δ_{HS} the HS state is essentially not populated for $T < T_{\text{MI}}$. This implies that below T_{MI} the susceptibility data of LaCoO_3 are described within a LS/IS model and above T_{MI} within a LS/IS/HS model. Therefore, we have also fitted $\chi_{\text{Co}}(T)$ of our $\text{La}_{1-x}\text{Eu}_x\text{CoO}_3$ samples separately above and below T_{MI} by the susceptibility of two- and three-state models. However, in particular within the three-state model, there are so many parameters that physically meaningful results can be obtained only if a well justified model about the nature of the metal-insulator transition and/or the expected changes of the energies of the various spin states are used.

In order to keep the number of parameters small we decided to restrict ourselves to two-state models and will present a description of $\chi_{\text{Co}}(T)$ within a LS/IS scenario with temperature-dependent energy gap as follows. An additional reason why we do not use the three-state model is that the splitting between different spin states is typically of the order of $1 \text{ eV} \simeq 12000 \text{ K}$.¹⁶ The small splitting between the LS and IS states ($\Delta \simeq 200 - 2000 \text{ K}$) observed in $\text{La}_{1-x}\text{Eu}_x\text{CoO}_3$ already requires a fine tuning of parameters. Thus it appears quite natural to assume that the HS state is located well above the other two spin states. Once we have fixed the model in this way, it is straightforward to derive the temperature dependence $\Delta(T)$ by writing Eq. 3 in the form

$$\Delta(T) = T \cdot \ln \left[\frac{N_{\text{A}} g^2 \mu_{\text{B}}^2 S(S+1)}{3k_{\text{B}}T} \frac{\nu(2S+1)}{\chi(T)} - \nu(2S+1) \right]. \quad (4)$$

Initially we tried to use the g factors of Table IV obtained from the susceptibility fits well below T_{MI} with temperature independent energy gaps in order to derive the energy dependence $\Delta(T)$ for larger temperatures. However, for $g < 2.4$ the argument of the logarithm in Eq. (4) becomes negative above about 500 K. Therefore we have used $g = 2.4$ for all samples and obtained the temperature-dependent energy gaps shown in Fig. 6.⁴² For $x \leq 0.5$ we have used $\nu = 1$ and find a moderate temperature dependence of $\Delta(T)$ in the low-temperature range. The average values $\langle \Delta(T) \rangle$ for $T < 400 \text{ K}$ are close to the values obtained from the fits with temperature-independent Δ [see Table IV]. This further justifies the fits of $\chi_{\text{Co}}(T)$ within the LS/IS scenario in the low-temperature range. For $x \geq 0.75$ we use $\nu = 3$ (as in the fits of $\chi_{\text{Co}}(T)$) and find some tendency to saturation only for $x = 0.75$, but not for EuCoO_3 . Thus, for $x \geq 0.75$ we can give only lower boundaries of $\Delta(T)$, which are so large that the obtained low-temperature values of $\chi_{\text{Co}}(T)$ are smaller than our experimental uncertainty. So far the $\Delta(T)$ curves for $x \geq 0.75$ do not contradict the LS/IS scenario for the low-temperature range.

At higher temperatures the $\Delta(T)$ curves strongly decrease for all samples. This decrease sets in when the

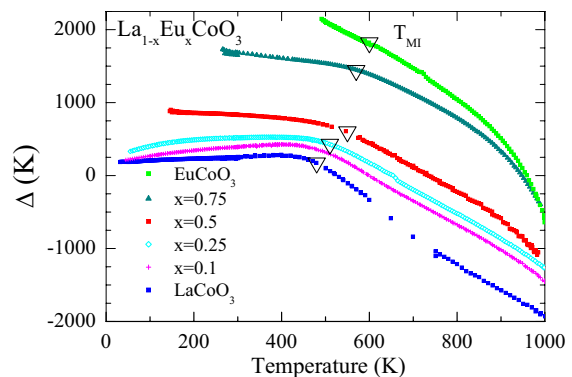


FIG. 6: Temperature dependence of the energy gaps Δ between the LS and the IS states obtained from Eq. 4 using $\nu = 1$ for $x \leq 0.5$ and $\nu = 3$ for $x \geq 0.75$ and $g = 2.4$ for all x . (see text)

metal-insulator transition is approached and is present up to 1000 K. A possible interpretation of the strong decrease of Δ around T_{MI} is that due to the metal-insulator transition the IS state is lowered in energy and is finally located well below the LS state. Within this interpretation the continuous decrease of $\Delta(T)$ up to the highest temperatures is not expected. One should, however, keep in mind that the application of Eqs. (3) and (4) is questionable in the conducting state above T_{MI} , because these equations are based on a model with localized moments. Note that this problem is also present for the three-state models.

One may suspect that a temperature-dependent energy gap could resolve the problem that on the one hand ESR data of LaCoO_3 propose a thermal population of a spin-orbit coupled HS state with $\dot{j} = 1$ and $g \simeq 3.5$,¹⁹ while on the other hand the susceptibility data are not at all reproduced by a population of such a state with a temperature-independent gap. Therefore we also calculated $\Delta(T)$ using these values in Eq. (4). For LaCoO_3 this leads to a continuously increasing energy gap from $\Delta(T < 40 \text{ K}) \simeq 200 \text{ K}$ to $\Delta(1000 \text{ K}) \simeq 1400 \text{ K}$ interrupted by a plateau of Δ from $500 \text{ K} < T < 600 \text{ K}$, i. e. the temperature dependence of Δ roughly resembles that of $1/\chi$. With increasing Eu content $\Delta(1000 \text{ K})$ remains essentially unchanged, because $\chi(1000 \text{ K})$ is almost constant, but the temperature dependence of Δ continuously decreases until $\Delta(T)$ is roughly constant for $x = 0.75$ and finally decreases with increasing temperature for $x = 1$. Because there is no reason why the temperature dependence of Δ should change so drastically as a function of Eu content, we do not consider this complex $\Delta(T, x)$ scenario as physically meaningful.

In conclusion, the analysis of the susceptibility data of $\text{La}_{1-x}\text{Eu}_x\text{CoO}_3$ reveals that a good description is possible within a LS/IS scenario below the metal-insulator transition. We find a drastic increase of the energy of the IS state with increasing Eu content and that for all Eu concentrations the metal-insulator transition is ac-

accompanied by an increase of the susceptibility of about $5 \cdot 10^{-4}$ emu/mole. This increase either indicates a strong decrease of the energy of the IS state around T_{MI} , or that a model of localized spins is no longer applicable above T_{MI} . It remains to be clarified whether $\chi_{\text{Co}}(T)$ above T_{MI} has to be described by local moments or not.

V. SUMMARY

We have studied the influence of chemical pressure on the spin-state transition and on the metal-insulator transition of LaCoO_3 by partially substituting the La^{3+} by the smaller Eu^{3+} ions. On the one hand the Eu substitution drastically influences the activation energy for charge transport in the insulating phase, which increases from about 1200 K in LaCoO_3 to about 3200 K in EuCoO_3 . The transition temperature of the metal-insulator transition, on the other hand, shows only a moderate change from about 480 K in LaCoO_3 to about 600 K in EuCoO_3 . Contrary to the metal-insulator transition, the spin-state transition is shifted very strongly towards higher temperatures with increasing Eu content as is observed independently in thermal expansion as well as in magnetic susceptibility measurements of $\text{La}_{1-x}\text{Eu}_x\text{CoO}_3$. Both quantities fulfill a simple scaling relation for $x \leq 0.25$ and $T \leq 180$ K. The experimentally obtained scaling factors agree very well with the value expected for a thermal population of the IS state without orbital degeneracy. Within this LS/IS scenario the experimental susceptibility data below about 450 K are satisfactorily reproduced for $x \leq 0.5$, whereas for larger x an orbital degeneracy of $\nu = 3$ yields a better

description. The lack of orbital degeneracy for $x \leq 0.5$ is an indirect evidence of orbital order, or a JT effect, between the thermally excited Co^{3+} ions in the IS state. For $x \geq 0.75$ this effect seems to play a minor role. This may arise from two effects which both act against an orbital/JT ordering: the spin-state transition occurs (i) at higher absolute temperatures and (ii) closer to the metal-insulator transition. With increasing Eu content we find a drastic increase of the energy splitting between the LS and the IS state from about 190 K in LaCoO_3 to about 2200 K in EuCoO_3 . As a consequence the population of the IS close to T_{MI} is very different for both compounds: $\approx 70\%$ in LaCoO_3 and $\approx 25\%$ in EuCoO_3 . This difference clearly shows that the occurrence of the metal-insulator transition is not related to the population of the IS state. So far the metal-insulator transition and the spin-state transition are decoupled from each other. The fact that for all Eu concentrations the susceptibility increases by about $5 \cdot 10^{-4}$ emu/mole around the metal-insulator transition and approaches a doping-independent value for $T \rightarrow 1000$ K indicates that nevertheless a common spin state, or combination of spin states, is approached well above T_{MI} . The nature of this spin state remains, however, unclear at present.

Acknowledgments

We acknowledge fruitful discussions with M. Braden, J. B. Goodenough, M. Grüninger, E. Müller-Hartmann, D. Khomskii, and L. H. Tjeng. This work was supported by the Deutsche Forschungsgemeinschaft through SFB 608.

-
- ¹ G. Jonker and J. V. Santen, *Physica* **XIX**, 120 (1953).
² P. Raccah and J. Goodenough, *Phys. Rev.* **155**, 932 (1967).
³ V. Bhide, D. Rajoria, G. R. Rao, V. Jadhao, and C. Rao, *Phys. Rev. B* **6**, 1021 (1972).
⁴ K. Asai, O. Yokokura, N. Nishimori, H. Chou, J. M. Tranquada, G. Shirane, S. Higuchi, Y. Okajima, and K. Kohn, *Phys. Rev. B* **50**, 3025 (1994).
⁵ M. Itoh, I. Natori, S. Kubota, and K. Motoya, *J. Phys. Soc. Japan* **63**, 1486 (1994).
⁶ M. A. Korotin, S. Y. Ezhov, I. V. Solovyev, V. I. Anisimov, D. I. Khomskii, and G. A. Sawatzky, *Phys. Rev. B* **54**, 5309 (1996).
⁷ R. H. Potze, G. A. Sawatzky, and M. Abbate, *Phys. Rev. B* **51**, 11501 (1995).
⁸ T. Saitoh, T. Mizokawa, A. Fujimori, M. Abbate, Y. Takeda, and M. Takano, *Phys. Rev. B* **55**, 4257 (1997).
⁹ K. Asai, A. Yoneda, O. Yokokura, J. M. Tranquada, G. Shirane, and K. Kohn, *J. Phys. Soc. Japan* **67**, 290 (1998).
¹⁰ S. Yamaguchi, Y. Okimoto, and Y. Tokura, *Phys. Rev. B* **55**, 8666 (1997).
¹¹ Y. Kobayashi, N. Fujiwara, S. Murata, K. Asai, and H. Yasuoka, *Phys. Rev. B* **62**, 410 (2000).
¹² M. Senaris-Rodríguez and J. Goodenough, *J. of Sol. State Chem.* **116**, 224 (1995).
¹³ Y. Tokura, Y. Okimoto, S. Yamaguchi, H. Taniguchi, T. Kimura, and H. Takagi, *Phys. Rev. B* **58**, 1699 (1998).
¹⁴ S. Yamaguchi, Y. Okimoto, H. Taniguchi, and Y. Tokura, *Phys. Rev. B* **53**, 2926 (1996).
¹⁵ C. Zobel, M. Kriener, D. Bruns, J. Baier, M. Grüninger, T. Lorenz, P. Reutler, and A. Revcolevschi, *Phys. Rev. B* **66**, 020402 (2002); see also C. Zobel, M. Kriener, D. Bruns, J. Baier, M. Grüninger, T. Lorenz, P. Reutler, and A. Revcolevschi, *Phys. Rev. B* **71**, 019902 (2005).
¹⁶ S. Sugano, Y. Tanabe, and H. Kamimura, *Multiplets of Transition-Metal Ions in Crystals* (Academic Press, New York and London, 1970), 1st ed.
¹⁷ P. G. Radaelli and S.-W. Cheong, *Phys. Rev. B* **66**, 94408 (2002).
¹⁸ I. A. Nekrasov, S. V. Streltsov, M. A. Korotin, and V. I. Anisimov, *Phys. Rev. B* **68**, 235113 (2003).
¹⁹ S. Noguchi, S. Kawamata, K. Okuda, H. Nojiri, and M. Motokawa, *Phys. Rev. B* **66**, 94404 (2002).
²⁰ D. Louca, J. L. Sarrao, J. D. Thompson, H. Röder, and G. H. Kwei, *Phys. Rev. B* **60**, 10378 (1999).
²¹ G. Maris, Y. Ren, V. Volotchaev, C. Zobel, T. Lorenz, and

- T. T. M. Palstra, Phys. Rev. B **67**, 224423 (2003).
- ²² Although orbital order and JT effect differ in their driving forces, an experimental distinction is extremely difficult or even impossible because both effects are strongly coupled to each other. In any material, orbital order will be accompanied by a lattice distortion which lowers the symmetry of the crystal field and enhances the splitting between the orbitals. Vice versa, a collective JT effect gives rise to a spatial ordering of the occupation of the orbitals.
- ²³ M. Kriener, C. Zobel, A. Reichl, J. Baier, M. Cwik, K. Berggold, H. Kierspel, O. Zabara, A. Freimuth, and T. Lorenz, Phys. Rev. B **69**, 094417 (2004).
- ²⁴ R. Pott and R. Schefzyk, J. Phys. E – Sci. Instrum. **16**, 444 (1983).
- ²⁵ J. C. Burley, J. F. Mitchell, and S. Short, Phys. Rev. B **69**, 054401 (2004).
- ²⁶ S. R. English, J. Wu, and C. Leighton, Phys. Rev. B **65**, 220407 (2002).
- ²⁷ R. Mahendiran and A. K. Raychaudhuri, Phys. Rev. B **54**, 16044 (1996).
- ²⁸ Since for the Eu-doped samples the resistivities above T_{MI} amount up to 100 m Ω cm one could label this transition an insulator-insulator transition. However, there is no qualitative change of the high-temperature transitions as a function of x . Thus we still label this a metal-insulator transition as it is usually done in the case of LaCoO₃.
- ²⁹ S. Yamaguchi, Y. Okimoto, and Y. Tokura, PRB **54**, R11022 (1996).
- ³⁰ The low-temperature value of the van Vleck susceptibility of the Co³⁺ ions (χ_{vV}^{Co}) is two orders of magnitude smaller than that of the Eu³⁺ ions. Thus, χ_{vV}^{Co} is expected to be constant in the examined temperature range, since due its smaller absolute value the temperature dependence of χ_{vV}^{Co} should also set in at much larger temperatures than that of χ_{vV}^{Eu} , which starts to decrease above about 100 K.
- ³¹ H. van Vleck, *The Theory of Electric and Magnetic Susceptibilities* (Oxford University Press, 1965).
- ³² We mention that this result does practically not change, when we use different temperature intervals for the fit, e.g. 4 K < T < 200 K or 4 K < T < 400 K.
- ³³ From the fits in the doping range $0.5 \leq x \leq 1$ we have found 457 K $\leq \Delta_{Eu} \leq$ 473 K and fixed this parameter to $\Delta_{Eu} = 460$ K for smaller x .
- ³⁴ K. Asai, O. Yokokura, M. Suzuki, T. Naka, T. Matsumoto, H. Takahashi, N. Mōri, and K. Kohn, J. Phys. Soc. Japan **66**, 967 (1997).
- ³⁵ T. Vogt, J. A. Hriljac, N. C. Hyatt, and P. Woodward, Phys. Rev. B **67**, 140401(R) (2003).
- ³⁶ M. Itoh, M. Mori, S. Yamaguchi, and Y. Tokura, Physica B **259-261**, 902 (1999).
- ³⁷ M. Itoh, J. Hashimoto, S. Yamaguchi, and Y. Tokura, Physica B p. 281&282 (2000).
- ³⁸ Because of the lower value of χ_0 of LaCoO₃ the present fit of the susceptibility data yields a g factor of 2.28 compared to $g = 2.13$ used in Ref. 15. As one consequence the expected scaling factors C , which are proportional to g^2 , increase by about 15% compared to the values given in Table I of Ref. 15, e.g. from $\simeq 167$ emuK/mole to $\simeq 192$ emuK/mole for the LS/IS scenario without orbital degeneracy. Another consequence is that increasing the orbital degeneracy from $\nu = 1$ to $\nu = 3$ is not sufficient anymore to explain the enhanced susceptibility above T_{MI} .
- ³⁹ In Ref. 15 we have used the thermal expansion of the charge-carrier doped La_{0.82}Sr_{0.18}CoO₃ as α_{bg} (dashed line in Fig. 4), which is somewhat larger than the α_{bg} used here. Since α of LaCoO₃ is much larger than both choices of α_{bg} , this uncertainty does hardly change $\Delta\alpha$ of LaCoO₃ (upper solid and dashed line in the lower panel of Fig. 4). Thus, the conclusions about the spin-state transition of LaCoO₃ discussed in Ref. 15 remain unchanged.
- ⁴⁰ T. Kyōmen, Y. Asaka, and M. Itoh, Phys. Rev. B **67**, 144424 (2003).
- ⁴¹ According to Refs. 9,17 the energy gaps decrease with increasing temperature above about 400 K, whereas Ref. 40 reports an increase of the energy gaps with increasing temperature starting already around 50 K.
- ⁴² Note that the Co³⁺ susceptibility is expected to vanish exponentially for $T \ll \Delta$ within any model discussed so far. Experimentally, $\chi_{Co}(T)$ is obtained from the raw data by subtracting χ_{bg} (see Eq. 1 and Fig. 5). Therefore $\chi_{Co}(T)$ scatters around zero below a certain temperature and we can derive $\Delta(T)$ only for temperatures where $\chi_{Co}(T)$ is significantly larger than the scatter around zero.
- ⁴³ S. Stølen, F. Grønvdold, H. Brinks, T. Atake, and H. Mori, Phys. Rev. B **55**, 14103 (1997).